

PERIOD ANALYSIS OF 3 ECLIPSING BINARY STARS WITH TESS DATA

DZYGUNENKO, ANDRII¹, TVARDOVSKYI, DMYTRO²

- 1) Astronomical Observatory, Taras Shevchenko National University of Kyiv, 3 Observatorna St., 04053 Kyiv, Ukraine, andridzigunenko@gmail.com
- 2) Centennial Centre for Interdisciplinary Science, Department of Physics, University of Alberta, Edmonton, Alberta, Canada T6G 2E1, dmytro.tvardovskyi@gmail.com

Abstract: We studied three eclipsing binary systems: TIC 199716496, TIC 414764074, and TIC 435447013, using TESS space telescope photometric data. We classified the first and the third stars as Algol-type variables and the second star as W Ursae Majoris. We calculated the periods and initial epochs for all three objects and later corrected them using O-C curve analysis. Further investigation revealed a significant reflection effect in TIC 435447013, and possible star spots in TIC 414764074. Moreover, TIC 199716496 appeared to have strange semiregular period changes. These findings enhance our understanding of binary systems despite raising even more questions about the nature of observed features of variable stars.

Keywords: eclipsing binary stars – period analysis – O-C curve – reflection effect

1 Introduction

Eclipsing binaries are a significant class of astronomical objects consisting of a pair of stars that are gravitationally bound to each other and orbit around a common center of mass. Binary stars are much more numerous than other types, comprising about 75% of all stars (Raghavan et al., 2010), but only a small percentage of these are eclipsing variables. Their fundamental features facilitate research; for instance, binary stars are periodic, as their orbital period is determined solely by their masses and the distance between them. Provided that no internal or external processes alter the masses of the stars or dimensions of their orbits, the period remains unchanged for millions of years. Additionally, both stars' orbits lie in the same plane, which may have random orientations in space.

For eclipsing binaries, the variability period corresponds exactly to the orbital period. The light curve of an eclipsing binary exhibits several distinct features, including four extrema: two maxima, usually of the same magnitude, and two minima that often show significantly different depths. If the orbits of the stars are circular, the minima are separated by exactly 50% of the period. The deeper minimum is usually referred to as the primary minimum, while the other is the secondary minimum.

Although many eclipsing binary stars have variability periods that remain stable within the margin of error, some show significant period changes. Various mechanisms can cause observed periods to change in specific patterns, with these effects becoming apparent through long-term observations. For instance, mass transfer between components leads to a steady increase or decrease in period, while the presence of a third component (either

a star or a large exoplanet) results in cyclic period changes. To study long-term period changes, one can employ an O-C curve.

The O-C curve, or O-C diagram, is a plot with the moments of each individual extremum along the X-axis and the difference between the observed and calculated moments of extrema along the Y-axis. Despite slight scatter due to measurement errors, the points on the O-C diagram form a curve. If this curve is a line, it indicates an error in the period value. If the curve is parabolic, the period changes steadily at a constant rate. If it is cyclic, the period also changes in a cyclical manner.

For our study, we utilized photometric observations from the TESS Space Telescope. The TESS (Transiting Exoplanet Survey Satellite) mission, developed by NASA, is designed to discover exoplanets using the transit method. TESS observes the sky in sectors, each covering a specific region of 24 by 96 degrees for 27.4 days. Due to the specific configuration of sectors, some objects near the ecliptic poles are observed in more than 30 sectors. Each sector includes from 10 to 20 thousand stars with apparent magnitudes ranging from 2 to 17. The signal-to-noise ratio varies based on the magnitude of each individual star. TESS observations are freely accessible at the Mikulski Archive for Space Telescopes (MAST) (MAST, 2024). In this research, we utilized a specific format of observations labeled as “lightcurve,” which has an exposure time of 120 seconds. We worked with the PDCSAP_FLUX data product, meaning the flux was corrected beforehand. The PDCSAP_FLUX light curves also adjust for the amount of flux captured by the photometric aperture and contributions from nearby known stars.

We selected three eclipsing binaries for investigation: TIC 199716496¹, TIC 414764074², and TIC 435447013³. These stars caught our attention because they have not been studied thoroughly before and exhibit a variety of intriguing effects.

TIC 199716496 has a magnitude of 10.34 in the V band and is located at coordinates (RA: 16:57:33.88, Dec: +59:31:51.85). This system exhibits changing maxima and varying minima, indicating potential starspot activity or pulsations of one of its components.

TIC 414764074 has a magnitude of 8.49 in the V band and is located at coordinates (RA: 00:30:20.75, Dec: +16:35:15.04). This binary is particularly interesting due to signs of possible mass transfer between its components, based to the shape of the light curve.

TIC 435447013 has a magnitude of 10.34 in the V band and is situated at coordinates (RA: 23:08:06.64, Dec: +65:36:33.02). This system is noteworthy for its strong reflection effect.

For the objects studied in this research — TIC 199716496, TIC 414764074, and TIC 435447013 — we found observations spanning twenty-four, three, and two sectors, respectively. The specific sector numbers are listed in Table 1.

¹<http://cdsportal.u-strasbg.fr/?target=TIC%20199716496>

²<http://cdsportal.u-strasbg.fr/?target=TIC%20414764074>

³<http://cdsportal.u-strasbg.fr/?target=TIC%20435447013>

Table 1: All sectors used in the analysis for three eclipsing binary systems.

TIC ID	TESS sectors used
199716496	14-26, 40, 41, 47-60, 73-81
414764074	42, 43, 57
435447013	57, 58

2 Methods and analysis

2.1 Data processing, periods and O-C curves

Plotting O-C curves consists of several stages. The first step is to determine the observed moments of extrema. Traditionally, only the moments of minima are used for binary stars, but improvements in observation quality now allow for precise calculations of maxima timings as well. For this study, we used both minima and maxima to plot the O-C curves.

To calculate the moments of minima and maxima, we employed the software MAVKA (Andrych et al., 2020). This software approximates the parts of the light curve near extrema using several specialized functions for eclipsing binaries, returning the results with the smallest errors. In our research, we applied the symmetrical polynomial, wall-supported parabola (WSP), and Algol variable (NAV) methods to all the stars. However, due to the asymmetric maxima of TIC 435447013, the parabolic spline method was specifically used for this star.

Given the large number of extrema, we developed a Python script, SPLITTER, to divide the light curve into individual intervals, ensuring that each interval satisfied the following criteria:

1. Interval contains exactly one extremum.
2. Interval does not contain parts of other extrema.
3. Interval has no large gaps in observations.
4. Interval has at least 10 points for approximation.

A single sector of TESS observations, separated by SPLITTER, is shown in Figure 1. After pre-processing by Splitter, each extremum is approximated by MAVKA. As a result, we get timing and errors for each extremum.

The next step is to make an initial estimation of the variability period. Since this value will be corrected later, at this stage we need relatively accurate estimates. In this study, we determined the period using periodograms, more specifically - Lomb-Scargle method (VanderPlas, 2018), already implemented in ASTROPY library for Python 3.9. The variability period corresponds to the highest peak at the resulting curve, and since our stars are binary, this method gives us a half-period. Thus, we doubled it. Example of the periodogram is shown in Figure 2.

The final step is to calculate values of O-C with the following formula (Sterken, 2005):

$$O - C = t - (T_0 + N \cdot P). \quad (1)$$

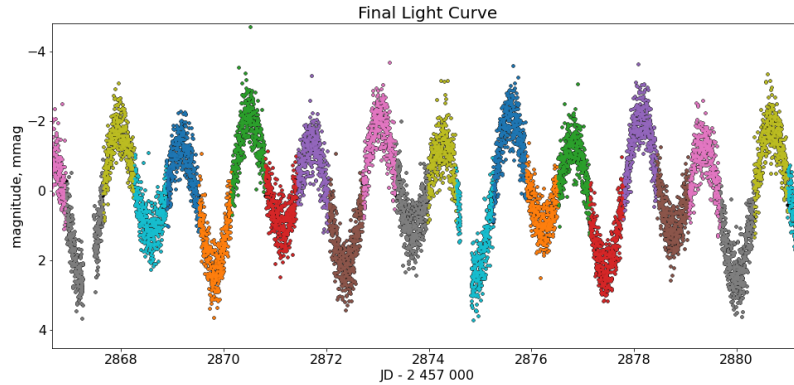


Figure 1: Part of a sector of TESS observations for eclipsing binary system TIC 414764074 separated using Splitter, different colour represents a separate interval. Black intervals are skipped because they don't meet the criteria.

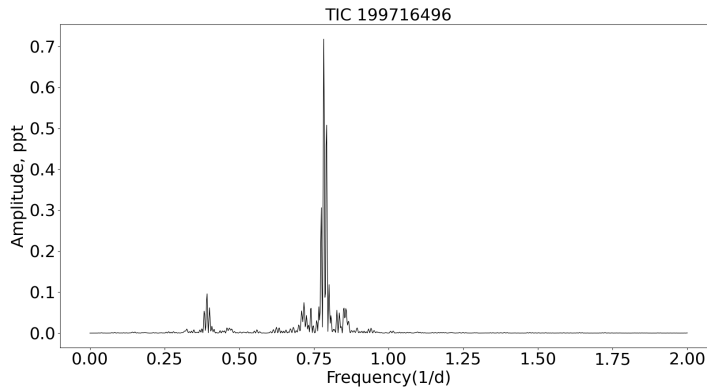


Figure 2: Periodogram for TIC 199716496

Here N – the integer number of complete cycles (variability periods) between the initial epoch and the observed minimum, usually called cycle number. It is calculated as follows:

$$N = \left[\frac{t - T_0}{P} \right] \quad (2)$$

$O - C$ is the observed minus calculated value, t is the observed moment of extremum, T_0 is the initial epoch, and P is the variability period. This specific formula is written for primary minima. For secondary minima, 0.5 must be added to N and for maximum – either 0.25 or 0.75, depending on its position. As initial epoch we initially used Julian Date of 2570000, which will also be corrected at the next stage.

2.2 Period and initial epoch correction

$O - C$ curves for all three stars are straight lines or curves with a linear trend, at least on the interval of observations that is currently available. Thus, we used them to correct

our first estimates of the period and initial epoch. Linear O-C curves were approximated with a simple formula for a line:

$$O - C = k \cdot t + b \quad (3)$$

Here k and b are coefficients of this line.

We determined the ephemeris using both the calculated periods and the observed times of extrema. Although standard linear regression methods, which are commonly used to fit minima timings, are straightforward, we chose a different approach that incorporates both maxima and minima into the analysis. This method helped improve our period corrections and allowed us to account for asymmetries in some of the systems, which standard fitting methods might miss.

Therefore, we plotted the moments of extrema (t) along the Y-axis instead of the cycle number (N), which is usually plotted. It doesn't affect the overall shape of the O-C curve or the values of the parameters within the margins of their errors. However, it is more practical because the observed moments of minima are fixed by definition. Cycle numbers, as well as calculated moments of minima, on the other hand, must be re-calculated every time we make even a slight correction of the period or initial epoch.

In this specific coordinates the correction to the period is calculated using the formula:

$$P_{new} = P_{estimated} \cdot (1 + k) \quad (4)$$

After period correction, we recalculated the values of O-C. Now the linear trend is gone, O-C curve is being approximated again, except this time the coefficient k equals to zero. Thus, equation 3 transforms into:

$$O - C_{new} = b_{new} \quad (5)$$

This means the O-C or its trend is now a horizontal line. To correct the initial epoch, we added this coefficient b_{new} to T_0 .

For calculating the errors of P_{new} and T_0 , we utilized the covariance matrix derived from the least-squares fit of the O-C diagram. The covariance matrix used for calculating errors was obtained using the `curve_fit` function in the `scipy.optimize` module of the SciPy library (SciPy Developers, 2020). This function implements a non-linear least-squares fitting algorithm and provides statistically consistent estimates for the fitted parameters and their uncertainties. The uncertainties in the slope k and intercept b were calculated as:

$$\Delta k = \sqrt{\text{cov}(k, k)}, \quad \Delta b = \sqrt{\text{cov}(b, b)}. \quad (6)$$

The uncertainty in the corrected period is then given by:

$$\Delta P = P_{new} \cdot \Delta k, \quad (7)$$

and the uncertainty in the corrected initial epoch is:

$$\Delta T_0 = \Delta b. \quad (8)$$

This error calculation method effectively accounts for the scatter in the observed data and provides reliable uncertainty estimates for the corrected periods and initial epochs. The results for all three stars, including the corrected periods, initial epochs, and their uncertainties, are summarized in Table 2.

3 Physical Phenomena

3.1 Reflection effect

After basic analysis of O-C curves and correcting both the period and initial epoch, we analyzed some interesting effects in stars. TIC 435447013 shows a significant reflection effect. This effect appears when two stars are separated by relatively small distances (usually by several stellar radii) and have considerable differences in surface temperatures. In this case, radiation from the hotter star creates a bright spot on the surface of the colder one. This spot is located in the region of the colder star closest to its hotter companion, as shown in Figure 3.

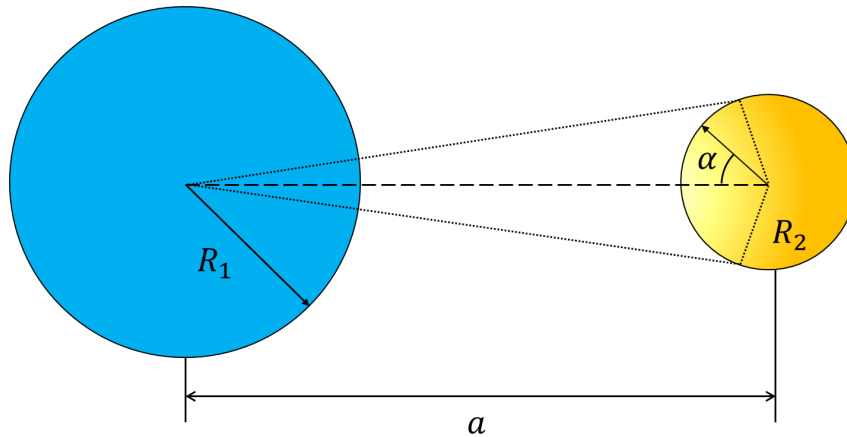


Figure 3: Schematic illustration of reflection effect and its geometry. Long dashed lines are tangents from the center of the hot star to the surface of the cold one. Parameters of the hot star have an index 1, and ones of the cold star have an index 2.

On the light curve, it is observed as a noticeable elevation of the secondary minimum and significant asymmetry of the maxima, which are both twisted towards the secondary minimum. As an example, we plotted a phase curve of TIC 435447013, as shown in Figure 4. In this case, moments of minima are located at the joints of the secondary minimum and maxima.

At the close orbital distances typical of tidally locked stars, these stars usually rotate along circular orbits, which means the temperatures of any point on their surfaces remain the same. To estimate the parameters of this hot spot, we need to know the geometry of the system and surface temperatures of both stars.

The temperature of the spot can be approximated as:

$$T_{spot}^4 \approx T_2^4 + T_1^4 \frac{R_1^2}{2a^2} \quad (9)$$

Phase Curve and Light Curve for TIC 435447013

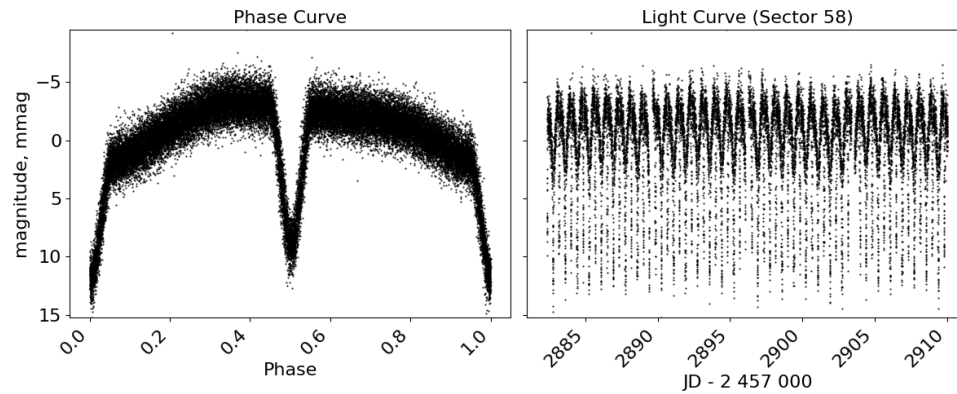


Figure 4: Phase curve and light curve (Sector 42) for TIC 435447013. Phase curve was plotted based on data from 2 sectors of TESS.

While we have made certain assumptions about the parameters of the spots, such as their sizes and temperature differences, we recognize that these assumptions may be overly simplistic. To address this, we plan to explore physical modeling in future research. This approach will allow us to better understand the complexities of spot dynamics and their impact on the light curves of the systems we studied.

3.2 Starspots

In this subsection, we discuss the star spot, which is clearly visible on the light curve of TIC 414764074, as well as on the phase curve, as shown in Figure 5, as its maxima differ significantly in apparent magnitude. Starspots may have various sizes and differences in

Phase Curve and Light Curve for TIC 414764074

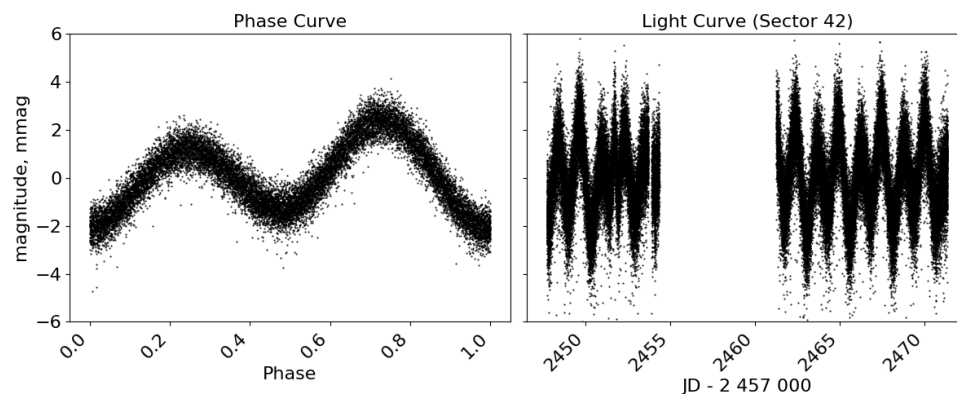


Figure 5: Phase curve and light curve (Sector 42) for TIC 414764074. The phase curve was plotted based on data from 3 sectors in total. The maximum, which comes right after the secondary minimum, appears lower than the other maximum.

temperature with another surface of the star. They also have different locations on the surface. For example, if even the large spot is located in the same position as the bright spot discussed in the previous subsection, it will be barely detectable. If the spot is on the side of a star, as shown in Figure 6, it has the most noticeable effect on the light curve.

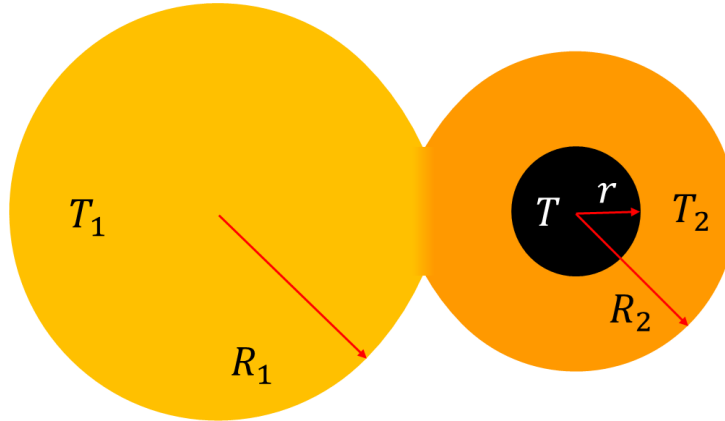


Figure 6: To make estimations of spot parameters for TIC 414764074, we assumed the position of the starspot on the side of the cold star. The shapes of both stars and the spot are simplified.

The maximum effect of the spot is determined by its size and temperature differences and could be roughly estimated using formula:

$$\frac{r^2}{R_2^2} \left(1 - \frac{T^4}{T_2^4} \right) = 1 - 10^{-\frac{\Delta m}{2.5}} \quad (10)$$

Here Δm is the magnitude difference between magnitude of maxima, T is the temperature of the spot, r is its radius. R_2 and T_2 correspond to the radius and surface temperature of the star where the spot is located. However, we have limited data in a single photometric filter, so we are unable to calculate the parameters of the spot separately.

4 Results and discussion

In this section, we present and discuss the results obtained from our study of the variable stars TIC 414764074, TIC 435447013, and TIC 199716496. We outline their classifications, calculated periods, initial epochs, and notable behaviors observed in their light curves, along with a complete analysis of their O-C curves.

We are planning to submit a comprehensive data table to VizieR following the publication of this article, which will include exact JD timings of extremes for all three eclipsing binaries in this study, along with JD errors and types of extremes, specifying whether they are minima or maxima, as well as primary or secondary.

4.1 Classification

Two stars, namely TIC 414764074 and TIC 435447013 were not classified as variable stars before. The eclipsing binary TIC 199716496 was already known and listed as EA

Table 2: Periods and initial epochs for three researched stars

TIC ID	Alternative ID	Period (days)	T_0 (JD)
199716496	RX J1657.5+5931	$1.04583737 \pm 0.00000002$	$2457000.05559 \pm 0.00006$
414764074	HD 2655	2.54673 ± 0.00006	2456999.7 ± 0.06
435447013	TYC 4286-373-1	0.83252 ± 0.00001	2457000.19 ± 0.02

type binary/X-ray source (Devor et al., 2008). We confirmed the classification of TIC 199716496 as EA type variable, classified TIC 414764074 as EW type and classified TIC 435447013 as EA type.

4.2 Periods and initial epochs

As the result of O-C processing, we calculated the values of periods and initial epochs for all three stars. This research is part of a series of studies conducted by many contributors, and they are all dedicated to variable stars and TESS observations. If those stars are periodic and don’t show any steady period changes, we are able to choose any $T_0 + N \cdot P$ as the initial epoch, as long as N is an integer. Thus, we decided to unify initial epochs in this and further research instead of scattering them in the range of several thousand days. So, we kept initial epochs as close as possible to $JD = 2457000$. The corrected values of periods and initial epochs are provided in Table 2.

Our value of the period for TIC 199716496 almost perfectly matched the one, published in (Devor et al., 2008), which was calculated to be 1.046 days. Our one has higher accuracy, probably due to the larger dataset used. For two other stars, our values of periods have larger errors because of the relatively short data range.

4.3 TIC 199716496

Among all three stars, TIC 199716496 has seemingly the most standard EA-type phase curve. Phase curve for this variable star is presented in Figure 7. However, its shape changes noticeably even during a single 27-day sector. Changes became even more significant as we studied long-term variations. The shape of the maxima is constantly twisting and wiggling, while the minima remain seemingly unchanged. This change is noticeable by comparing the light curves from different sectors, for example, from sectors 19, 25, and 54, as shown in Figure 8.

The potential impact of de-trending on the changes observed in the light curve of TIC 199716496 was supposed to be during the review of this article. However, we must note that we did not apply any de-trending procedures to our data.

The behaviour of maxima is quite weird. From some parts of the light curve, it is clear that the star has a reflection effect. However, the reflection effect does not miraculously disappear after several days and then appear again. Between those “reflection” parts of the light curve, there are other ones which are similar to the light curves of the stars with large starspots. O-C curves provided us with even more information about light curve behaviour; see Figure 9. We made two separate plots. The first one contains only minima,

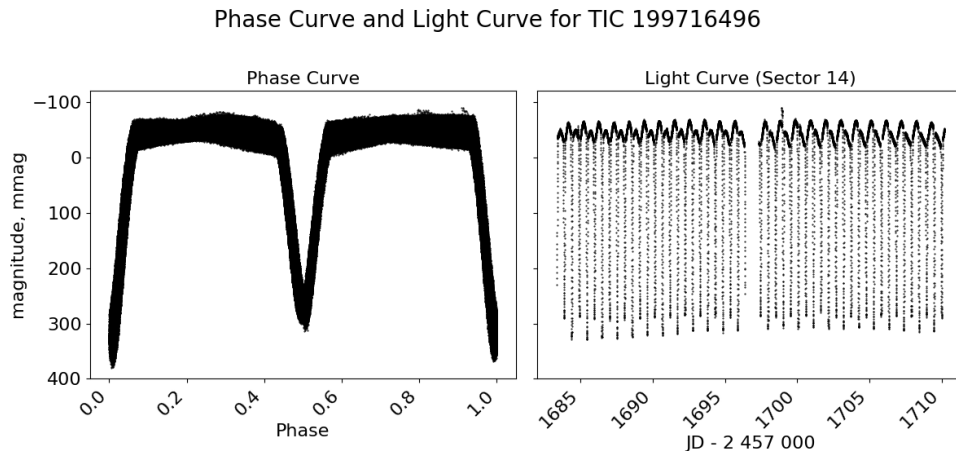


Figure 7: Phase curve and light curve (Sector 14) for TIC 199716496. The phase was curve plotted based on data from 26 available TESS sectors.

and the second one – only maxima. It is visible that both maxima and minima alter their position.

The observed changes in the light curve of TIC 199716496 are indeed present across all studied sectors, not limited to individual ones. These variations have been consistently detected in data from Sectors 14, 19, 25, and 54, with similar patterns in all cases. Moreover, such phenomena have been observed in other variable stars, suggesting they are real astrophysical signals rather than artefacts of the TESS pipeline or subsequent processing. For example, (Pan & Zhang, 2023) investigated KIC 7284688, a solar-type eclipsing binary observed with Kepler and TESS, which displayed a rapidly varying O’Connell effect – a phenomenon characterized by unequal maxima in the light curve.

Their analysis attributed these variations to starspot migration caused by differential rotation, further supported by periodic signals detected in both O-C curves. The changes in TIC 199716496’s light curve maxima, including the appearance and disappearance of reflection effects, might be explained similarly due to dynamic magnetic activity or spot modulation. The consistent detection of this variability across all TESS sectors supports its phenomenon rather than being an artefact of data reduction.

As it is clearly seen from the bottom plot in Figure 9, the position of both maxima of TIC 199716496 changes their shape in a very specific pattern. The position of both maxima changes almost perfectly in the antiphase. The shift between the position of both maxima and their expected positions oscillates from 0.09 to 0.45 days. The behavior is quasi-periodic, the shape of the O-C curve for minima nearly repeats itself every 90-120 days, whereas O-C for maxima repeats itself every 100-115 days also oscillating based on the period analysis in Figure 10. At the very end, those oscillations seemingly disappear, and both curves for maxima become seemingly stable. The stellar rotation period of about 100 days for TIC 199716496 is much longer than the orbital period of around 1 day. This difference suggests that the star’s rotation is unrelated to its orbital motion.

The top plot is even more intriguing. At the beginning of the plot, which corresponds to May 2019, both minima were cyclically shifting in phase. This pattern continues until the

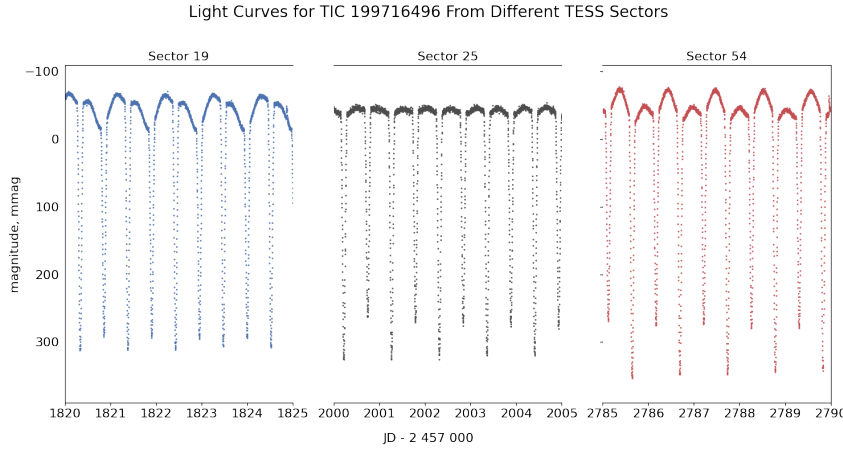


Figure 8: Observations from 3 sectors for TIC 199716496 showing different behaviour of the same star. The reflection effect is clearly visible in sector 19. The light curve from sector 25 looks like a regular light curve for an EA-type star without any features. Observations from sector 54 show a significant difference in the magnitude of maxima.

gap in August 2020 and later during June–August 2021. However, after the observations of this star continued in December 2021, that pattern completely broke, and O-C behaviour became seemingly chaotic, as can be clearly visible in Figure 11. In reality, those curves are not turning into a chaotic scatter of dots; they remain quasi-periodic, although the amplitude of the changes decreases.

The first half of O-C for minima might be explained by the presence of the light-time effect (LTE) and the third component in the system, as both stars orbit around the barycenter of this triple system (Sterken, 2005). However, the second part is completely uncharacteristic of LTE, as well as such behaviour of maxima. Thus, we completely rejected this hypothesis at the early stages of the research.

Another idea which might explain the shape of the O-C curve is the pulsations of one of the components. Such changes of light curve might correspond to pulsations with a period of about 100 days. However, O-C curves of binaries with long-period pulsations have different, more regular shapes, as shown in (Shi et al., 2021a).

The final hypothesis is the presence of the reflection effect (which creates a bright spot) and a large dark spot. This spot rotates with the star near its equator, and thus, for some time intervals, the positions of both bright and dark spots almost match. Despite it requires a combination of several infrequent phenomena, it explains several observed phenomena:

1. The reflection effect is sometimes cancelled by the dark spot, thus cyclically appearing and disappearing again on the light curve.
2. The parts of the light curve where maxima have some difference in magnitude are typical for stars with starspots.
3. The Lifespan of those dark spots is not eternal. For large spots, it is determined by the differential rotation of its star (Berdyugina, 2005). It explains constant changes

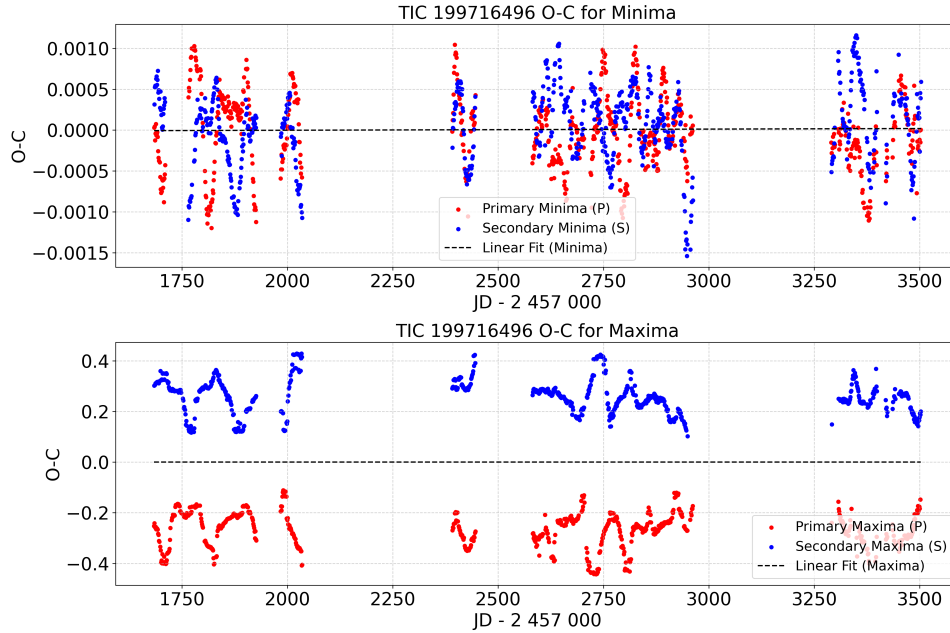


Figure 9: $O - C$ of minima (top panel) and maxima (bottom panel) for the star TIC 199716496.

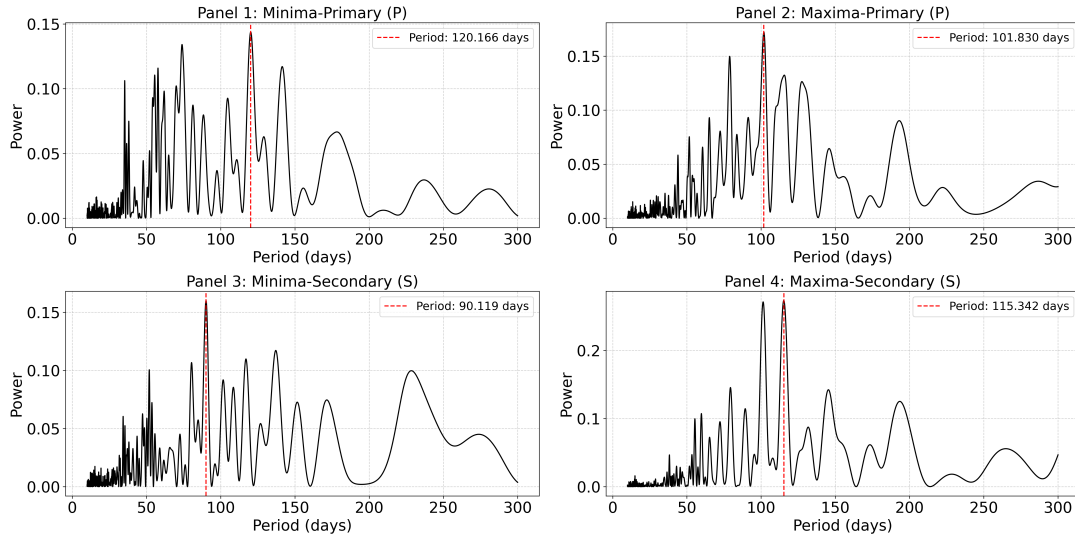


Figure 10: Fourier transform periodograms for the $O - C$ analysis of TIC 199716496, separated into four panels: (1) primary maxima, (2) secondary maxima, (3) primary minima, and (4) secondary minima.

of the “period” of $O - C$ oscillations as the spot is probably fragmented. It also gives a hint on the nature of the $O - C$ curve between $JD = 2459500$ and $JD = 2459900$, where the hypothetical spot was almost destroyed after several years of existence.

This explanation also requires both stars not to be tidally locked yet, so the dark spot could actually move relatively to the bright spot. Since they belong to EA type, not EB or EW, this is entirely possible, as well as stellar rotation periods between 80-120

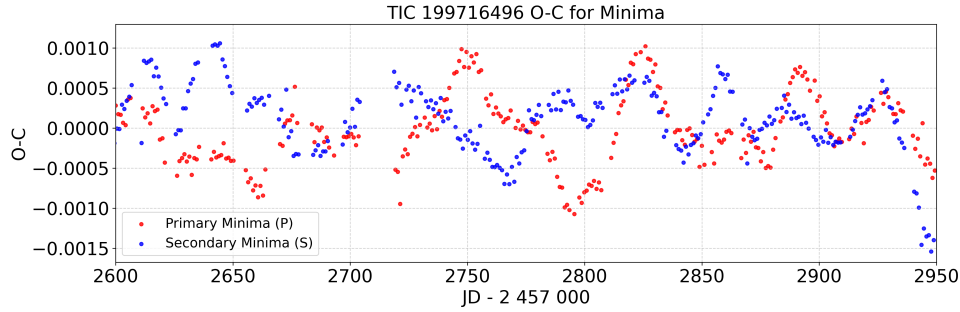


Figure 11: Zoomed final part of O-C curve for TIC 199716496.

days. Although this theory sounds complicated and thus highly controversial, (Shi et al., 2021b) studied a similar star and explained their findings based on a combination of the reflection effect and a dark spot. The O-C curve of that star also shows chaotic behaviour, although less complex than TIC 199716496. Moreover, it also has flares similar to those observed in TIC 199716496.

Then, we tried to estimate the bright spot's temperature and the dark spot's features at its prime in 2019. However, we could not find any open-access spectroscopic or at least multi-band photometric observations for this star to calculate any required parameters separately. The same lack-of-data issue was present with the two other eclipsing binaries we researched.

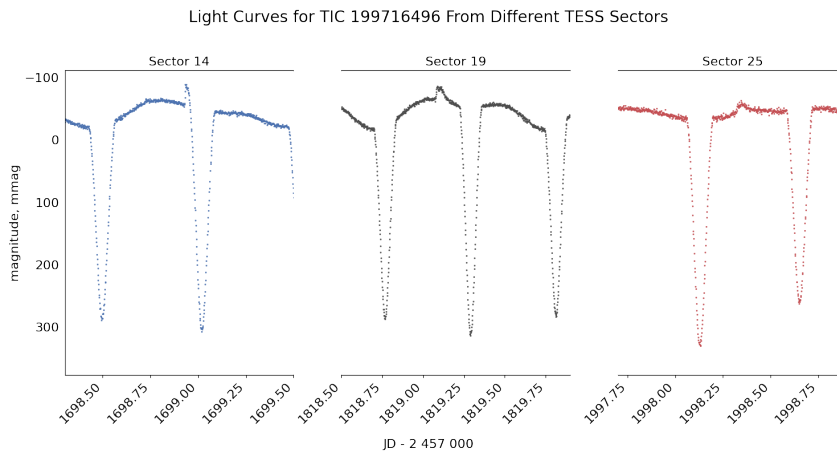


Figure 12: Several small flares of TIC 199716496 detected in sectors 14, 19, 25

Finally, we report observations of several non-periodic low amplitude flares in the light curve of TIC 199716496, as shown in Figure 12. In general, some flares detected in TESS data are false positives created by various issues with TESS photometry, and they are usually located at the very beginning or very end of the sector. However, those flares were in the middle of the corresponding sectors and thus must be real.

To ensure the integrity of our data, we carefully checked the quality flags using the `lc.quality` attribute from the Lightkurve library, confirming that there were no indica-

tors of incorrect data in the provided sectors. This validation suggests that these observations are likely genuine and not artefacts of the data collection process. Furthermore, the position of the Moon and the bright planets could not have affected these observations, as the coordinates for our object have a declination of $+59:31:51.85$. Notably, this high declination makes it improbable for other planets or the Moon to intersect and influence the light curve. The probable cause of these flares is magnetic reconnection, similar to that observed in solar flares.

The changes in the general shape of the light curve, including clearly visible variations in the height of the maxima, could also be caused by some type of physical phenomenon. They are definitely not a result of de-trending, since we did not use any de-trending operations in our algorithm. An alternative explanation of such changes are pulsations with long period of about 100 days of one of components.

4.4 TIC 414764074 and TIC 435447013

Both stars have a much smaller amount of data, and their O-C curves resembled straight lines without any signs of significant period changes. O-C curve for maxima of TIC 435447013, Figure 14, bottom panel), as it was expected, appeared to be two straight parallel lines because the maxima themselves are twisted towards the secondary minimum. That is obviously the result of the reflection effect.

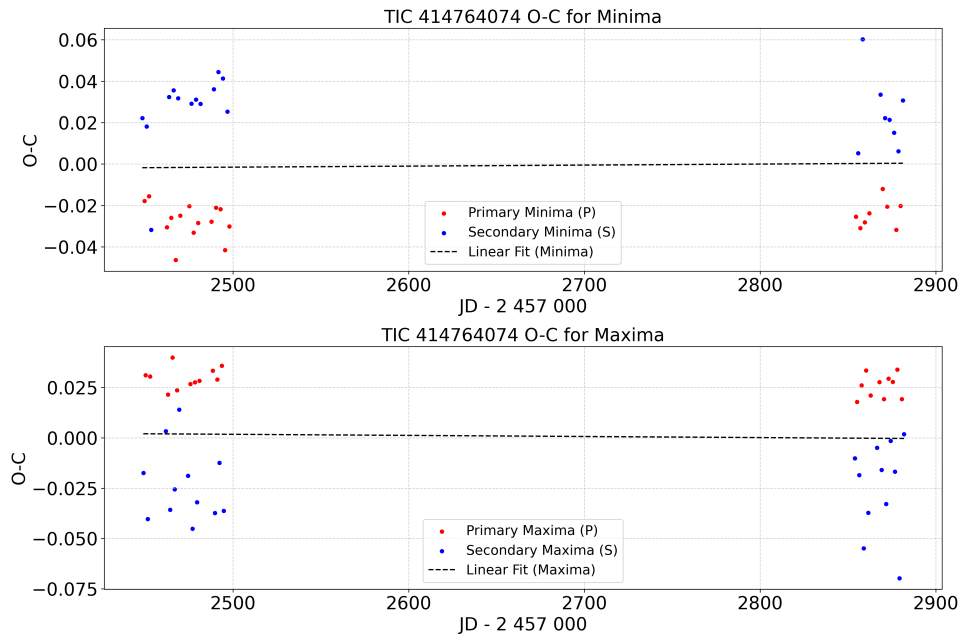


Figure 13: $O - C$ of minima (top panel) and maxima (bottom panel) for TIC 414764074.

The only noticeable feature to mention is a similar, but much smaller effect in both maxima and minima of TIC 414764074, Figure 13. As it appears in both types of extrema, it is most likely caused by slightly elliptical orbits of components in this system. We

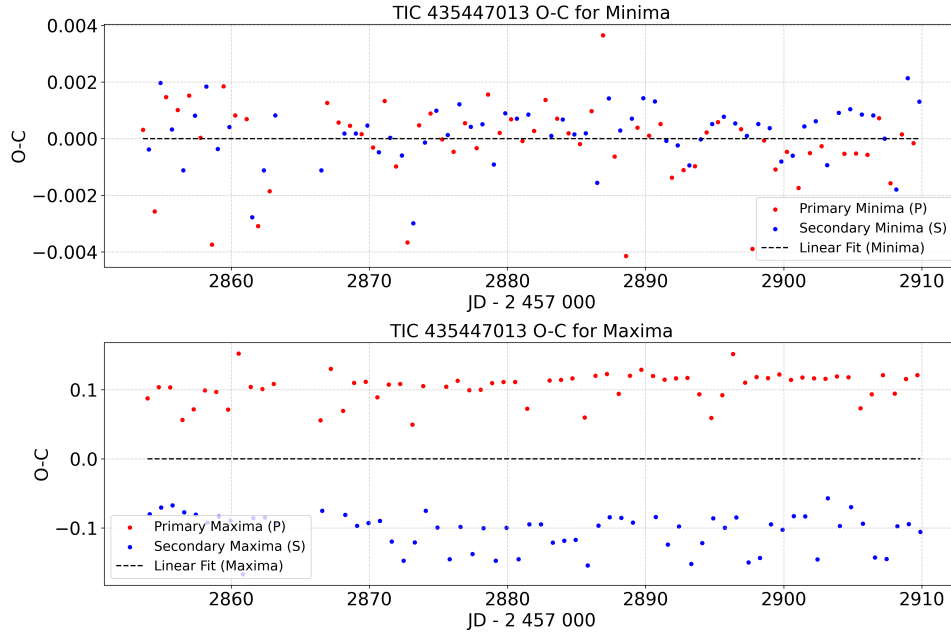


Figure 14: $O - C$ of minima (top panel) and maxima (bottom panel) for TIC 435447013.

estimated this eccentricity using the formula from (Tsevevich, 1973):

$$e \cdot \cos\omega = \frac{\pi \Delta t}{2 P} \quad (11)$$

Here e is eccentricity of the orbit, ω is argument of pericenter and Δt is the distance between those parallel lines on $O-C$. We get the result $e \cdot \cos\omega \approx 0.035$. However, due to the low signal-to-noise ratio, the relative error of those estimates should be significant. Except this slight eccentricity, $O-C$ curves for these two stars didn't show anything unusual.

5 Summary

We studied light curve variations and period changes of three eclipsing binary stars, each having its distinct features. TIC 199716496 was particularly interesting because of the unusual behavior of its $O-C$ curve, which we were able to explain with our findings.

For TIC 414764074, we observed evidence of a slight eccentricity in its orbit, which appeared as a systematic variation in both maxima and minima. The $O-C$ curve for this star showed straight lines, indicating stability in its period without significant changes.

TIC 435447013 also demonstrated a notable reflection effect, which affected its light curve symmetry. This reflection effect highlights the interaction between the binary components, suggesting that the stars are closely bound and influence each other's brightness.

Although our study primarily focused on these light curve behaviors, we recognize the importance of deriving physical parameters for these systems. For TIC 199716496, which has a visual magnitude of about 10^m , we plan ground-based follow-up observations. With multi-color photometry and spectroscopy, along with radial velocity measurements, we

could refine our understanding of this star and its companions. These measurements would help clarify our assumptions about TIC 199716496 and enable us to physical modelling for this binary, as well as calculate more parameters of the system.

We also plan to carry out ground-based observations of TIC 199716496 to test our ideas about this type of binary star.

The observed changes in TIC 199716496’s light curve, including the reflection effect and asymmetric maxima, may be explained by the O’Connell effect, which is often attributed to starspot activity or the interaction between the binary components. This effect might provide further insight into the underlying causes of the observed variations in the system.

Acknowledgements: We sincerely thank the TESS space telescope team and Mikulski Archive for Space Telescopes for providing free access to observations. This research was part of the TESS-UA-2022 project for young scientists, organized by Clear Skies Foundation. We are also grateful to Kateryna Andrych and Dr. Ivan Andronov for providing MAVKA software and Dr. Olena Shubina for discussions.

References

- Andrych, K. D., Andronov, I. L., & Chinarova, L. L. 2020, *Journal of Physical Studies*, 24(1), id. 1902, [2020JPhSt..24.1902A](#)
- Berdyugina, S.V. 2005, *Starspots: A Key to the Stellar Dynamo*. *Living Rev. Sol. Phys.* 2, 8
- Devor, J., Charbonneau, D., O’Donovan, F. T., Mandushev, G., & Torres, G. 2008, *AJ*, 135, 850-877, [2008AJ....135..850D](#)
- Mikulski Archive for Space Telescopes (MAST), https://archive.stsci.edu/tess/bulk_downloads.html
- Pan, Y., & Zhang, X. 2023, KIC 7284688: A Solar-type Eclipsing Binary with Rapidly Varying O’Connell Effect, *The Astronomical Journal*, 165, 247, [2023AJ....165..247P](#)
- Raghavan, D., McAlister, H. A., Henry, T. J., Latham, D. W., Marcy, G. W., Mason, B. D., ... ten Brummelaar, T. A. 2010, *ApJS*, 190(1), 1-42, [2010ApJS..190....1R](#)
- SciPy Developers. 2020, *curve_fit*: Non-linear Least Squares Minimization and Curve Fitting for Python, https://docs.scipy.org/doc/scipy/reference/generated/scipy.optimize.curve_fit.html
- Shi, X.-d., Qian, S.-b., Li, L.-j., & Liao, W.-p. 2021, HL Dra: an active Algol-like binary system with a pulsating component star and a cool third body, *MNRAS*, 505, 6166-6178, [2021MNRAS.505.6166S](#)
- Shi, X.-d., Qian, S.-b., Li, L.-j., & Liu, N.-p. 2021, Flaring and Spot Activities on the Semi-detached Binary System KIC 06852488, *AJ*, 161, id. 46, [2021AJ....161...46S](#)
- Sterken, C. 2005, *The Light-Time Effect in Astrophysics: Causes and Cures of the O-C Diagram*, *ASPC*, 335, 3, [2005ASPC..335....3S](#)
- Tsevech, Vladimir Platonovich, 1973, *Eclipsing variable stars*, New York, J. Wiley. [1973evs..book....T](#)
- VanderPlas, J. T. 2018, *ApJS*, 236(1), id. 16, [2018ApJS..236...16V](#)